ON FRAGMENTATION OF ALUMINUM PROJECTILE ON MESH BUMPERS

T.Shumikhin[3], A.Semenov[1], L.Bezrukov[1], A.Malkin[2], N.Myagkov[3], M.Kononenko[3]

(1) Federal Research Institute of Aviation Systems, ul. Victorenko 7, 125319 , Moscow, Russia, Email: semenov@gosniias.ru
(2) Institute of Physical Chemistry of RAS, Leninskiy prosp. 31, 119991, Moscow, Russia, Email: mlk@front.ru
(3) Institute of Applied Mechanics of RAS, Leninskiy prosp. 32a, 119991, Moscow, Russia, Email: tish2002@mail.ru

ABSTRACT

Presented results of tests in which 6.35–mm diameter (D_0) aluminum sphere projectiles impacted bumpers consist of single or several steel meshes. There were used two types of meshes with the parameter $\varepsilon = D_0 /(d_w+l) \sim 2$ for one type and $\varepsilon \sim 5$ for other one (d_w wire diameter and l mesh size). The thin and thick plates of aluminum alloy placed on path of debris have been used as witnesses to get data for mass distribution of fragments behind the bumpers. The type of fragmentation (character of craters or holes distribution on the witness surface) for the meshes of different type was found to be quite unlike. There is a big central leader and small fragments with wide lateral dispersion for mesh with $\varepsilon \sim 5$ and no central compact leader, but several similar big fragments for meshes with $\varepsilon \sim 2$. The relative distribution of mass is estimated.

1. INTRODUCTION

Meteoroids and orbital debris protection of spaceships is one of the most important safety problem for the manned spacecrafts. Efficiency of the meteoroids and orbital debris mesh protection has been shown in works of NASA Johnson Space Center (Christiansen, E.L., 1990, 1993, 1995). Rather detailed experiments, elucidating the integral dispersing and fragmentation properties of meshes due to their interaction with a projectile were carried out as well (Horz, F.,1995). However, for the mesh bumpers both experimental and numerical analysis of physical processes is not available in literature such widely as for the case of continuous bumpers (Grady, D.E., 1997; 2001; Piekutowski, A. J., 1997). It is qualitatively clear that in case of mesh bumper the process of fragmentation goes in quite different way then in case of continuous one because unloading and destruction of a projectile starts practically instantly from its frontal surface, after its interaction with a mesh.

A quantity of researches is necessary to find out the rational geometrical parameters of a mesh and the material of its elements.

How it was noted above, the shield protective structures consist of grids have not been studied enough. Earlier the foreign investigators applied only aluminum grids. Logically in this work it is to investigate grids made of other materials. Although the brass and steel grids are more massive than the aluminum ones but when a high velocity interaction occurs they lead to a greater extent of the impactor fragmentation than on an aluminum grid.

Note that these experiments has a prospecting character. But they are useful evidently. The experiments were made using steel grids.

In the "light"-weight protection structure the first bumper B_1 must provide a maximum effective fragmentation of the projectile (and optimal in sizes of the fragments) and a maximum angle of scattering. It can be done if the first bumper be optimal from this point of view because the projectile has the maximum kinetic energy at the first bumper.

It can be supposed that when an impact occurs two processes of crushing are available. The first of them is a shock-wave process (multiple scabbing) when the grid is close to the solid plate in its characteristics (ε~5). The second is an implantation process (of a wire into the projectile) which is available when $\varepsilon \sim$ 2-3 i.e. when the grids are rather massive.

To run initial experiments to evaluate influence of the grid parameters on the character and extent of the fragmentation a scheme with a single bumper and a relatively thick back wall spaced from the bumper with distance of 80 ÷ 250 mm is used. Fragmentation parameters determined using analysis of craters and holes on the rear wall (their sizes, distribution, scattering angle). The size of craters on thick rear wall plate was estimated as volume of semi-ellipsoid.

A projectile of aluminum alloy AD-1, d_0 = 6.35 mm is used. The incidence was normal.

Note that if there is not shown the distances between bumper's grids in a figure then the grids packed enough tightly. As criterions of the fragmentation extent the following parameters are accepted:

D - an average diameter of scatter region where craters greater than 1-mm size are available,

φ – an angle of the scattering of these fragments (evidently $\varphi = 2\, arctg(\, (D / 2) / S\,)$

2. EXPERIMENTAL RESULTS

2.1 Experiment with thin meshes (ε = 5.38)

Experiment C01 (Fig.1):

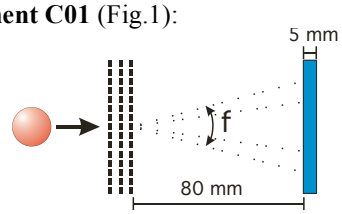

Experiment: C-01(evacuated chamber)
Projectile : Al Alloy Ball (AD-1), D_0=6.35mm
Bumper : 3 Steel Meshes 1.2 x 0.32 mm, G_B = 2.46 kg/m^2
Rear Wall : Al Alloy Plate (AMG-6), Thickness = 5 mm
Velocity : V_0=3,200 m/s

Figure 1. A scheme of the experiment C01

The damage of the RW (Figs. 2,3):

1. The hole has the sizes 9 ×13 mm; D= 114.7 mm, φ=71.27 degree, the area of the hole S_{C01}=155.52mm^2
2. On the schematic picture of the damage (Fig. 1) it is shown the hole and craters in the size from ~1.0 mm. In total such craters about 240. The largest of them have the size up to 5.0 mm

Figure 2. A photo of the surface of the back wall in the penetration region (C01)

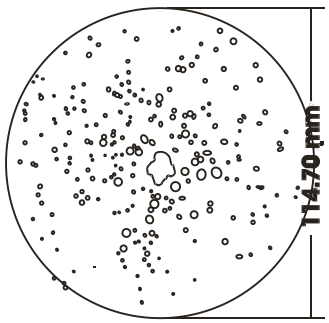

Figure 3. A location scheme of the hole and the craters greater 1mm in size (C01)

Experiment C02 (Fig.4):
In this experiment 4 layers of fabric (SVM in Russian marking; m = 0.15 kg/m^2) between meshes are placed

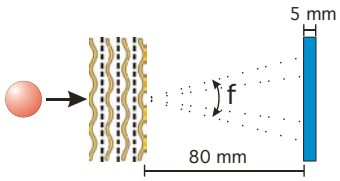

Experiment: C-02(evacuated chamber)
Bumper : 3 Steel Meshes 1.2 x 0.32 mm, 4 Layer of Fabric (SVM) G_B = 3.10 kg/m^2
Rear Wall : Al Alloy Plate (AMG-6), Thickness = 5 mm
Velocity : V_0=3,400 m/s

Figure 4. A scheme of the experiment C02

The damage of the RW (Figs. 2b, 2c):

1. The hole has the size ~ 9 mm; D= 105.01 mm, φ=66.55 degree, the area of the hole S_{C02}=159.67mm^2
2. In total there are about 174 of craters with size greater-equal ~1mm. The largest of them have the size up to 5.0 mm

Experiment C03 (Fig.5)

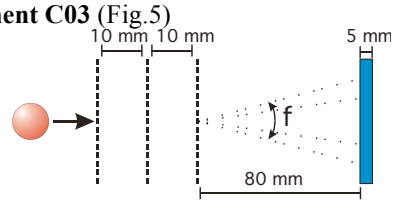

Experiment: C-03(evacuated chamber)
Projectile : Aluminum Ball (AD-1), D_0=6.35mm
Bumper : 3 Steel Meshes 1.2 x 0.32 mm, G_B = 2.46 kg/m^2
Rear Wall : Aluminum Plate (AMG-6), Thickness = 5 mm
Velocity : V_0=3,060 m/s

Figure 5. A scheme of the experiment C03

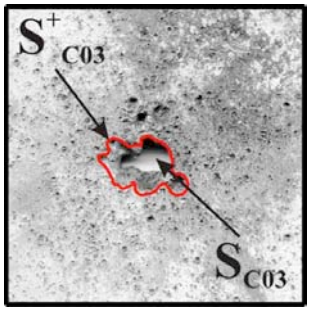

Figure 6. A photo of the surface of the back wall in the penetration region (C03)

The damage of the RW:

1. The hole has the sizes 9 ×13 mm; D=107.05 mm, φ = 67.6 degree, the area of the hole S_{C01}=52.24mm^2, the full area of the crater-like zone around the hole plus the area of the hole S^+_{C03}=139.72mm^2 (fig.6).
2. In total there are about 140 of craters with size greater-equal ~1mm. The largest of them have the size up to 5.0 mm

In the fig.7 is depicted the distribution of area of the central perforation holes for experiments C01,C02 and C03. It can be seen that the in the experiment C03 the area is noticeable smaller. Taking into consideration the form of the perforation hole's contours and decreasing of the hole area we can conclude that the central leader is not the whole fragment but the dense cloud of smaller fragments.

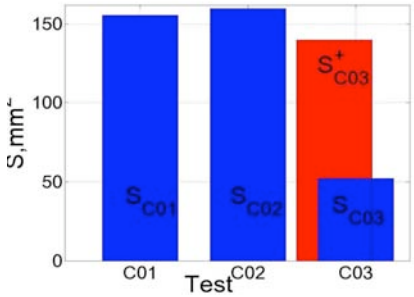

Figure 7. The area of the central perforation hole

Experiment C04 (fig.8)

The spatial distance and the RW thickness are increased up to 250 mm and 10 mm accordingly to get more distinct spaced craters of individual fragments. The thickness 10 mm (or more) of the rear wall plate allows to consider the formation of craters as to be in semi-infinity medium. So we could estimate the kinetic energy K_i of individual fragments using well known relation for the volume V_{crat} of impact craters (Balankin,A.,1990)

$$K_i \sim V_{crat} \qquad (1)$$

Assuming the velocity v_i of different fragments to be roughly equal we could get the distribution of fragment masses m_i. For estimation of proportion of the leading fragment mass M_L to the total mass M_t of all marked fragments we would use the parameter $\mu = M_L / M_t$

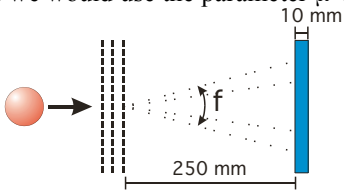

Experiment: C-04(evacuated chamber)
Projectile : Al Alloy Ball (AD-1), D_0=6.35mm
Bumper : 3 Steel Meshes 1.2 x 0.32 mm, G_B= 2.46 kg/m²
Rear Wall : Al Alloy Plate (AMG-6), Thickness = 10 mm
Velocity : V_0=3,500 m/s

Figure 8. A scheme of the experiment C04

The damage of the RW (Figs. 9, 10):

1. RW has a crater with diameter 12 mm and depth ~ 5мм. The RW underside has a scabbing with the size ~25 mm. D= 181.10mm; φ = 39.82 degree.
2. On the schematic picture of the damage (Fig. 10) it is shown the craters. In total craters in size grater-equal ~1 mm are about 230. The largest of them have the size up to 9.0 mm, about 10 craters has the size 4 – 6 mm.

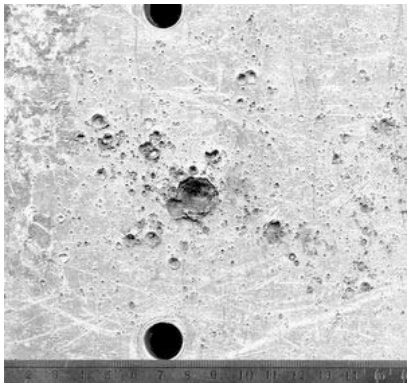

Figure 9. A photo of the surface of the rear wall in the penetration region (C04)

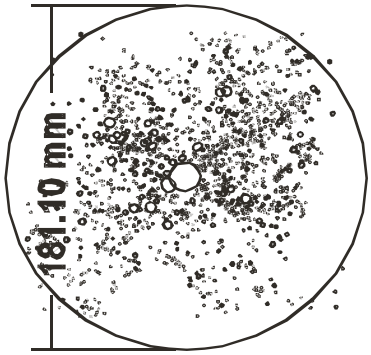

Figure 10. A location scheme of the craters on the rear wall (C04)

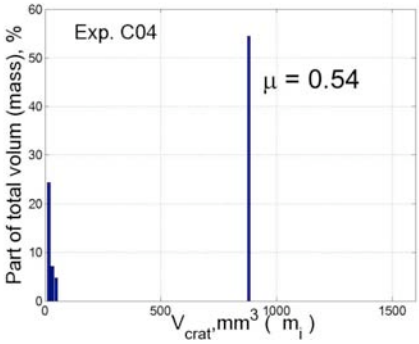

Figure 11. Distribution of crater volume (i.e. fragments masses) on the rear wall (C04)

In the fig.11 is presented the bar-graph of the distribution of crater volume (i.e. the distribution of fragment masses in the frame of above mentioned assumption). The X-direction corresponds to the volume of craters V_{cart} (formed with spaced intervals of size $V_L/100$) and the Y-direction corresponds to the part of total volume of the craters formed by fragments with mass from the spaced interval end defined by the relation

$$\left(\sum_{m_{i-1} < m_k \le m_i} m_k / M_t \right) 100\%$$

where M_t is considered as mass of all fragments.

2.2 Conclusion concerning experiments # C01-C04:

1. Three meshes, light in weight, as the first bumper provided good enough the fragmentation of projectile, however, there was the central leading fragment in the impact direction. Estimated mass of this fragment is no more than 54 % of the total fragment masses (i.e. μ=*0.54*).
2. The influence of spatial distance between meshes (0 -10 mm) or the presence of a fabric layer between the meshes on the projectile fragmentation is insignificant.

2.3 Experiment with heavy meshes ($\varepsilon < 2.5$)

A special series of experiments were dedicated to the investigation of the state of the fragments which arrange the central part of the cloud and pose the most threat to penetrate the back wall. The problem is to find out if the hole in the wall is a result of impact of a single fragment or it is a result of multi impact of several fragments moving closely together. If the last assumption is right than the air dynamic force can segregate these fragments.

For clarification 8 experiments were conducted under the normal atmosphere pressure (DZR01, DZR02, DZR03, DZR04, DZR05, DZR06, DZR07, DZR08). Dispersion of the fragments was fixed on rear wall. The RW was the plate of aluminum alloy (AMG6, in Russian marking) with thickness more than 15 mm (except DZR04 where the thickness of the rear wall was 3 mm). Fig.12 suggests the scheme of the experiments.

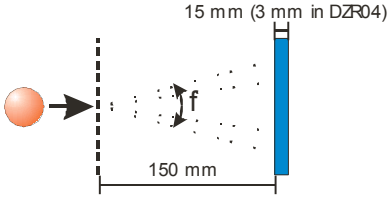

Experiments: DZR01, DZR02, DZR03, DZR 04, DZR 05, DZR 06 , DZR07, DZR08 (all in air)
Projectile : Al Alloy Ball (AD-1), D_0=6.35mm
Bumper : Steel Mesh
Rear Wall : Al Alloy Plate (AMG-6), Thickness = 15 mm (3mm in DZR04)

Figure 12. Scheme of the experiments DZR01-DZR08

In some of the experiments the grid was covered by teflon or polyethylene film. But the influence of the films was nor observed.
In the Fig. 12 below there are results of experiments DZR01-DZR08 with photos of rear wall and experiment parameters.

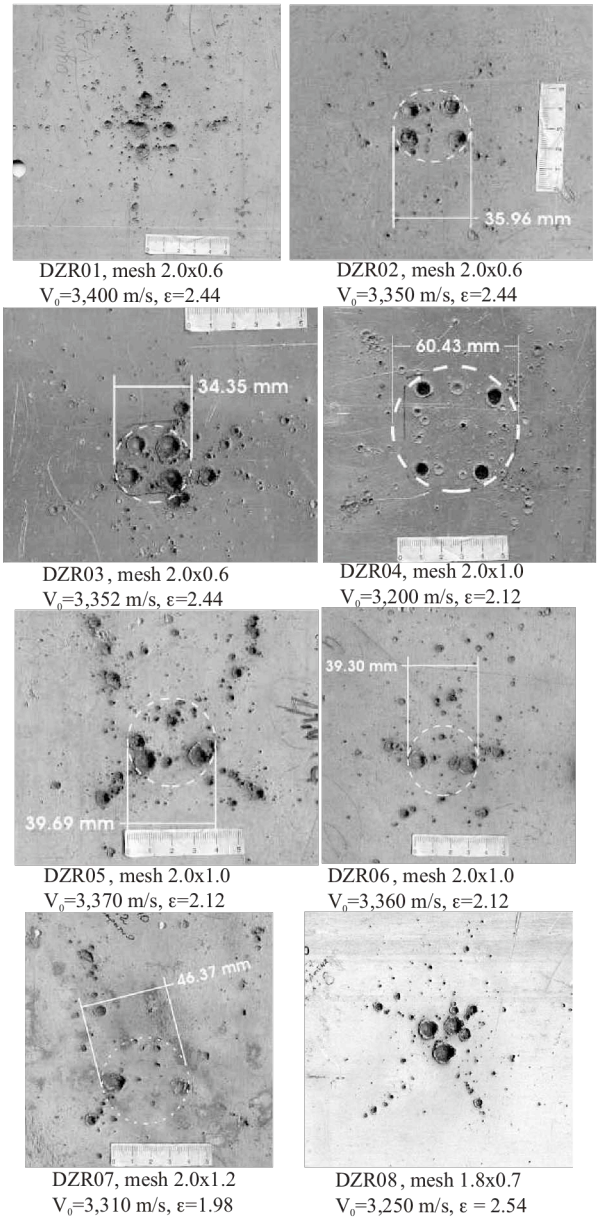

DZR01, mesh 2.0x0.6 V_0=3,400 m/s, ε=2.44
DZR02, mesh 2.0x0.6 V_0=3,350 m/s, ε=2.44
DZR03, mesh 2.0x0.6 V_0=3,352 m/s, ε=2.44
DZR04, mesh 2.0x1.0 V_0=3,200 m/s, ε=2.12
DZR05, mesh 2.0x1.0 V_0=3,370 m/s, ε=2.12
DZR06, mesh 2.0x1.0 V_0=3,360 m/s, ε=2.12
DZR07, mesh 2.0x1.2 V_0=3,310 m/s, ε=1.98
DZR08, mesh 1.8x0.7 V_0=3,250 m/s, ε = 2.54

Figure 13. Photos of the surface of the rear wall in the penetration region (DZR01-DZR08)

The presented photographs show that the leading most dangerous fragment acted on the rear wall as a whole one really may consist of several smaller fragments. Due to the action of the air the coarse fragments of a projectile become distinguishable. The parameter μ for these experiments was estimated for the 4 heaviest fragments.

Experiment DZR05
The damage of the RW:

1. The central zone of RW has four craters with diameter 7mm - 9 mm. The average diameter of this zone is D_L=*42.55 mm*, the angle is φ_L=*16.2* degree. The average distance of centre of the zone from the centre of these craters is ~ 20 mm.

2. The average diameter of scattering of fragments is on craters in $D=210.89mm$ (for craters with the size ≥ 1mm; $\varphi=70.2$ degree.
3. The quantity of the craters more than *1 mm* is about 210.
4. $\mu_1 = 0.20$; $\mu_2 = 0.13$; $\mu_3 = 0.10$; $\mu_4 = 0.08$

Experiment DZR06

The damage of the RW:

1. The central zone of RW has four craters with diameter 6 mm - 10 mm. Their scattering diameter is $D_L=32.14mm$, the angle is $\varphi_L=12.23$ degree.
2. The average diameter of scattering of small craters (~1mm) is $D=208.27mm$, the angle is $\varphi=69.54$degree.
3. The quantity of the craters more than 1 mm is about 120.
4. $\mu_1 = 0.25$; $\mu_2 = 0.23$; $\mu_3 = 0.06$; $\mu_4 = 0.05$

The parameter μ was estimate for all these experiments. In Fig. 14 is depicted the dependence of μ on the geometrical and weight parameters of mesh used in these experiments. It seems that the surface weight of the meshes don't influence on the μ.

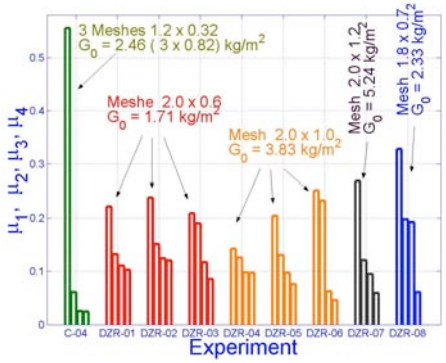

Figure 14. Dependence of μ on the mesh parameters

In the fig.15 presented three characteristic type of fragmentation observed in the experiments (one leading fragments, four leading fragments and two leading fragments) and the dependence of the type on the parameter ε.

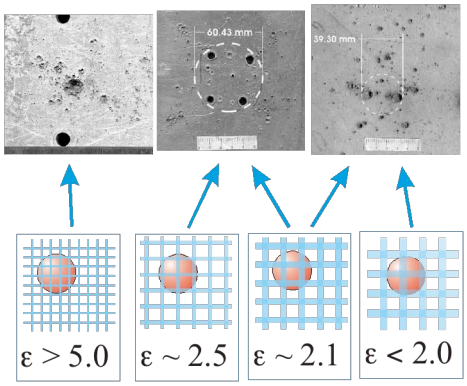

Figure 15. The dependence of fragmentation type on the parameter of ε

2.4 Conclusion concerning experiments # DZR01-DZR04

The analyze of the experiments show that the heavy meshes can provide the steady fragmentation of the projectile in which the parameter μ of the biggest of the leading fragment not exceed the value of $\mu = 0.25$ for the range of meshes with $\varepsilon \sim 2.1 - 2.5$ (at least for the interval of impact velocity *2,500 – 3,500 m/s*) . Also it seems that the geometrical parameter of meshes of such value of ε have more influence on mass distribution of leading fragments than mesh weight characteristic. Apparently in case of heavy meshes so called implantation mechanism of fragmentation prevails in contrast of scabbing mechanisms in case of continuous-like bumper. The implantation of wire into the body of projectile causes the appearance of disjoint forces leading to complete separation of coarse fragments. The geometrical parameter of the mesh seems to be a control parameter of the process. The mesh with geometrical (and may be material) parameters that provide the fragmentation that give the smallest parameter μ may be denominated as "optimized mesh" (for some effective size of projectile).

3. The possible ways for practical use of optimized meshes

To establish if there is some practical way to provide the lateral moving of leading fragments that occur after impact of projectile against some optimized mesh the following experiments were realized (fig. 16 and fig. 18).

Experiment BM08:

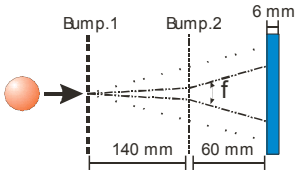

Experiment: BM-08(evacuated chamber)
Projectile : Ball, Al Alloy (AD-1), D_0=6.35mm
Bumper 1 : Steel Mesh 2.0 x 0.6 mm, G_{B1} = 1.71 kg/m^2
Bumper 2 : Steel Mesh 1.2 x 0.32 mm, G_{B2} = 0.82 kg/m^2
Rear Wall : Plate, Al Alloy (D16T), Thickness = 6 mm
Velocity : V_0=3,150 m / s

Figure 16. Scheme of the experiment BM08

The result:

The RW(Fig.17b) has a hole with diam.~1 mm.

The damage of Bump.2(Fig.17a):

The central hole (i.e. D_L) has diam.~15 mm. The average diameter is $D=113.18$ *mm,* the angle is φ= 44.0 degree. The angle of leading fragments φ_L= 6.*13* degree

The damage of the RW (Fig. 17):

1. The RW has 4 characteristic craters with diameters 5 - 8 mm in the central zone. The average diameter

of this zone is D_L=*32.69mm*, and its angle is φ_L= 9.*34* degree.

2. The average diameter of zone of small craters (with diameter ~1mm) is *D=147.71* mm, the angle of this zone is φ= *40.5* degree.
3. The quantity of the craters more than 1 mm is about 250.

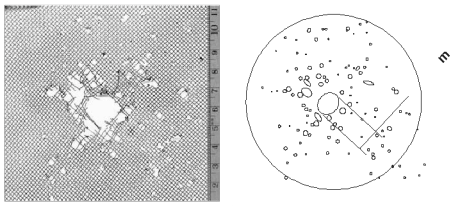

a) The photo and the scheme of the holes in Bumper # 2 (test BM08)

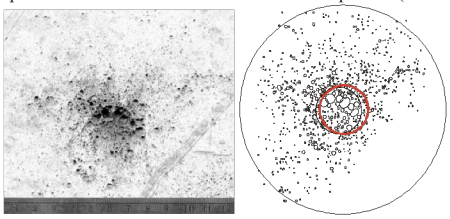

b) the damage photo of the RW and the scheme of RW craters (test BM08)

Figure 17. The damage on the Bumper#2 and RW

Obviously the φ_L on the RW increased because of the interaction with the second bumper. In the central area of RW can be spot evidently distinguishable craters of 4 leading fragments.

Experiment C112:

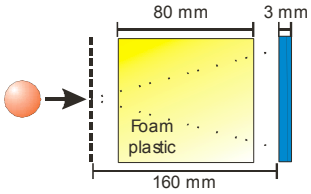

Experiment :C112 (evacuated chamber)
Projectile :Ball, Al Alloy (AD-1), D_0=6.35mm
Bumper :Steel Mesh 2.0 x 0.6 mm, G_0 = 1.71 kg/m^2
Foam Plastic:Thickness = 80 mm, G_F = 3.36 kg/m^2
Rear Wall :3 mm , Al-Ti (Double Layer), G_{RW} = 7.56 kg/m^2
Velocity :V_0=3,470 m / s

Figure 18. Scheme of the experiment C112

The damage of RW (Fig.19):

1. The RW has 6 characteristic craters (and holes on ballistic limited) with diameters 3mm - 4mm. The average diameter of this zone is D_L=*52.20mm*, and its angle is φ_L= 18.*53* degree.
2. Smaller craters in small quantity arranged around the craters of leading fragments.

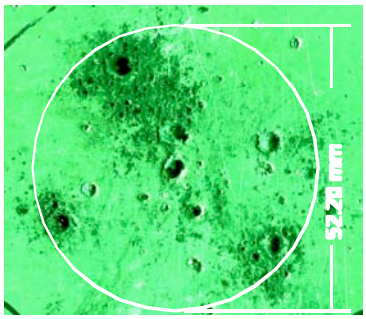

Figure 19. A photo of the surface of the rear wall in the penetration region (C112)

Like in the air the leading fragments have lateral displacement in the foam plastic.

ACKNOWLEDGEMENT

This work was supported from International Science and Technology Center (project #1917).

Christiansen, E.L., AIAA Paper No. 90-1336, 1990.

Christiansen, E.L. and Kerr, J.H., Int. J. Impact Engng, Vol. 14, 169-180, 1993

Christiansen, E.L., Crews, J.L. et al, Int. J. Impact Engng, Vol. 17, 217-228, 1995

Horz, F., Cintala, M.J. et al., Int. J. Impact Engng, Vol. 17, 431-442, 1995

Grady, D.E. and Kipp, M.E. Int. J. Impact Engng. Vol. 20, pp. 293-308, 1997

Grady, D.E. and Winfree, N.A., Int. J. Impact Engng., Vol. 26, 249-262 , 2001

Piekutowski, A. J., Int. J. Impact Engng., Vol. 17, 627-638,1995, Vol.20, 639-650, 1997

Balankin, A., Lubomudrov, A., Sevrukov, I., *Physics of the hyper-velocity impact*, Ministerstvo oborony SSSR, Moscow, 1990 (in Russian)